US 20150141874A1

(19) **United States**

(12) **Patent Application Publication**

Wilson

(10) **Pub. No.: US 2015/0141874 A1**

(43) **Pub. Date: May 21, 2015**

(54) **MULTI-BEAM ULTRASOUND DEVICE**

(71) Applicant: **Kitchener Clark Wilson**, Santa Barbara, CA (US)

(72) Inventor: **Kitchener Clark Wilson**, Santa Barbara, CA (US)

(21) Appl. No.: **14/082,541**

(22) Filed: **Nov. 18, 2013**

Publication Classification

(51) **Int. Cl.**

A61N 7/02	(2006.01)
A61B 5/00	(2006.01)
A61B 5/01	(2006.01)

(52) **U.S. Cl.**

CPC ... ***A61N 7/02*** (2013.01); ***A61B 5/01*** (2013.01); ***A61B 5/4836*** (2013.01); *A61N 2007/0078* (2013.01)

(57) **ABSTRACT**

A multi-beam ultrasound device with intersecting beams is presented for use in medical therapy and industry. Multiple ultrasound beams interfere constructively and destructively depending on their phase at the target tissue, and this device and its methodology uses phase control for intensity enhancement at the beam intersection. Two among many embodiments are detailed: phase matching where the phases of the beams are determined and controlled to be equal, and phase sweeping where the phases of the beams are purposely varied.

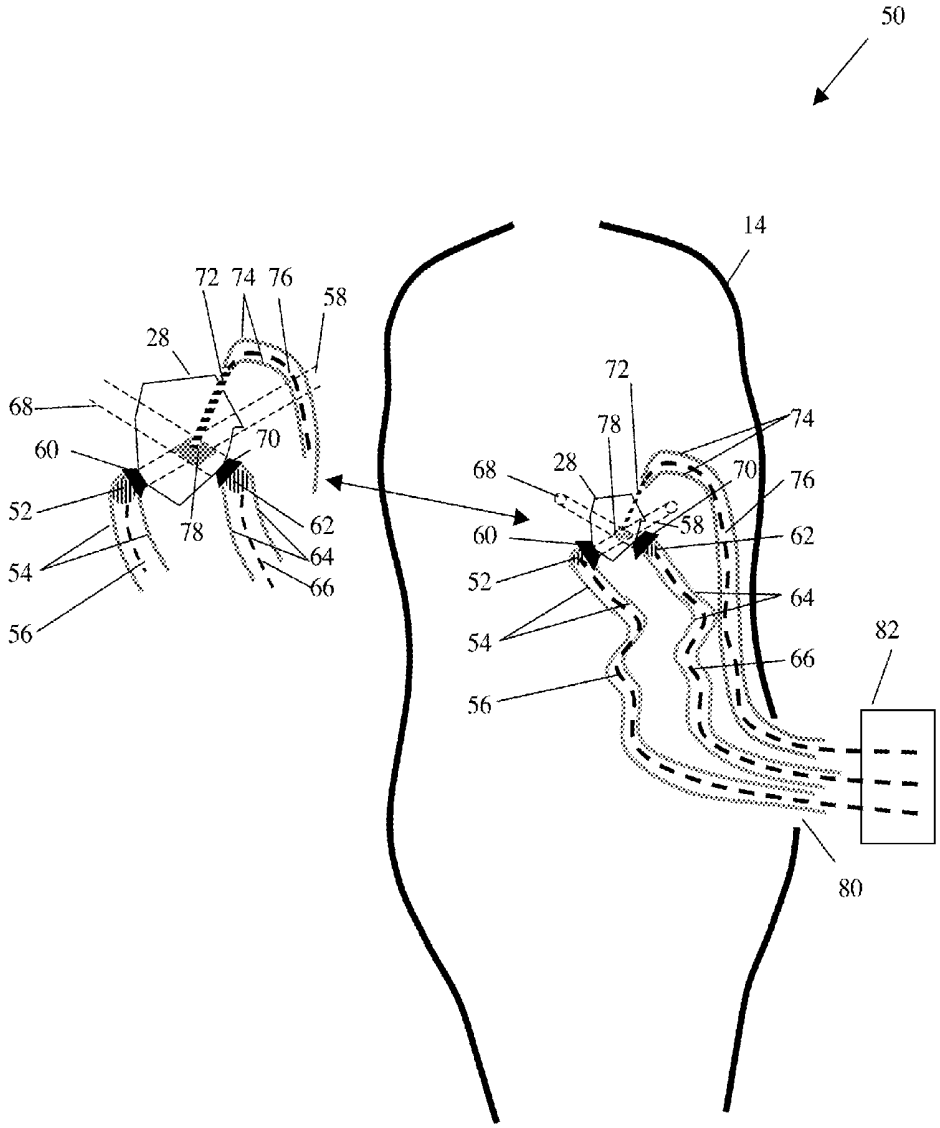

aperture diameter in cm: D

frequency in Mhz: f

speed sound in cm/sec: s

wavelength in cm: $\lambda = 10^{-4}\frac{s}{f}$

half – power attenuated distance in cm: $d_{half} = \frac{3}{\alpha f}$

3db beam width in cm: $w = 0.2568D$

beam divergence angle: $\sin(\beta/2) = 0.514\frac{\lambda}{D}$

near field distance in cm: $N \approx \frac{D^2}{4\lambda} - \frac{\lambda}{4}$

TBL 1

			1 MHz frequency		10 MHz frequency	
Material	α attenuation (db/Mhz/cm)	s sound speed (m/s)	λ wavelength (cm)	d half power attenuation (cm)	λ wavelength (cm)	d half power attenuation (cm)
Air	160	330	0.033	0.02	0.0033	0.002
Blood	0.2	1570	0.157	15.00	0.0157	1.500
Bone		4080	0.408		0.0408	
trabecular	9.94			0.30		0.030
cortical	6.9			0.43		0.043
Brain	0.6	1540	0.154	5.00	0.0154	0.500
Breast	0.75			4.00		0.400
Cardiac	0.52			5.77		0.577
Connective tissue	1.57			1.91		0.191
Dentin	80			0.04		0.004
Enamel	120			0.03		0.003
Fat	0.48	1450	0.145	6.25	0.0145	0.625
Liver	0.5	1570	0.157	6.00	0.0157	0.600
Marrow	0.5			6.00		0.600
Muscle	1.09	1580	0.158	2.75	0.0158	0.275
Tendon	4.7			0.64		0.064
Soft tissue	0.54	1540	0.154	5.56	0.0154	0.556
Water	0.0022	1480	0.148	1363.64	0.0148	136.364

TBL 2

α (db/Mhz/cm)	s (m/s)	d half-power (cm)	f (Mhz)	λ (cm)	D (cm)	type	w width (cm)	β divergence angle (°)	N near field distance (cm)
0.54	1540	5.56	1	0.154	0.1	cardiac catheter	0.026	104.7	
					0.2	cardiac catheter	0.051	46.6	0.026
					0.3	laparoscopy trocar	0.077	30.6	0.108
					0.4	laparoscopy trocar	0.103	22.8	0.221
					0.5	laparoscopy trocar	0.128	18.2	0.367
					0.6	laparoscopy trocar	0.154	15.2	0.546
					0.7	laparoscopy trocar	0.180	13.0	0.757
					0.8	laparoscopy trocar	0.205	11.4	1.000
					0.9	laparoscopy trocar	0.231	10.1	1.276
					1	laparoscopy trocar	0.257	9.1	1.585
					1.1	laparoscopy trocar	0.282	8.3	1.926
					1.2	laparoscopy trocar	0.308	7.6	2.299
					1.3	laparoscopy trocar	0.334	7.0	2.705
					1.4	laparoscopy trocar	0.360	6.5	3.143
					1.5	laparoscopy trocar	0.385	6.0	3.614
					1.6	laparoscopy trocar	0.411	5.7	4.117
					1.7	laparoscopy trocar	0.437	5.3	4.653
					1.8	laparoscopy trocar	0.462	5.0	5.221
					1.9	laparoscopy trocar	0.488	4.8	5.822
					2	laparoscopy trocar	0.514	4.5	6.455
water		test transducer							
0.0022	1480	1363.64	1	0.148	1.9	laparoscopy trocar	0.488	4.6	6.061

TBL 3

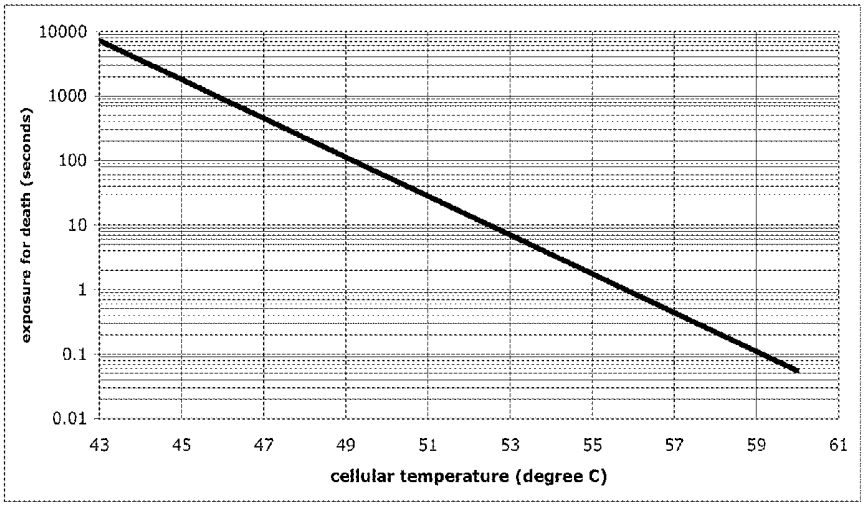

FIG 1
EXISTING ART

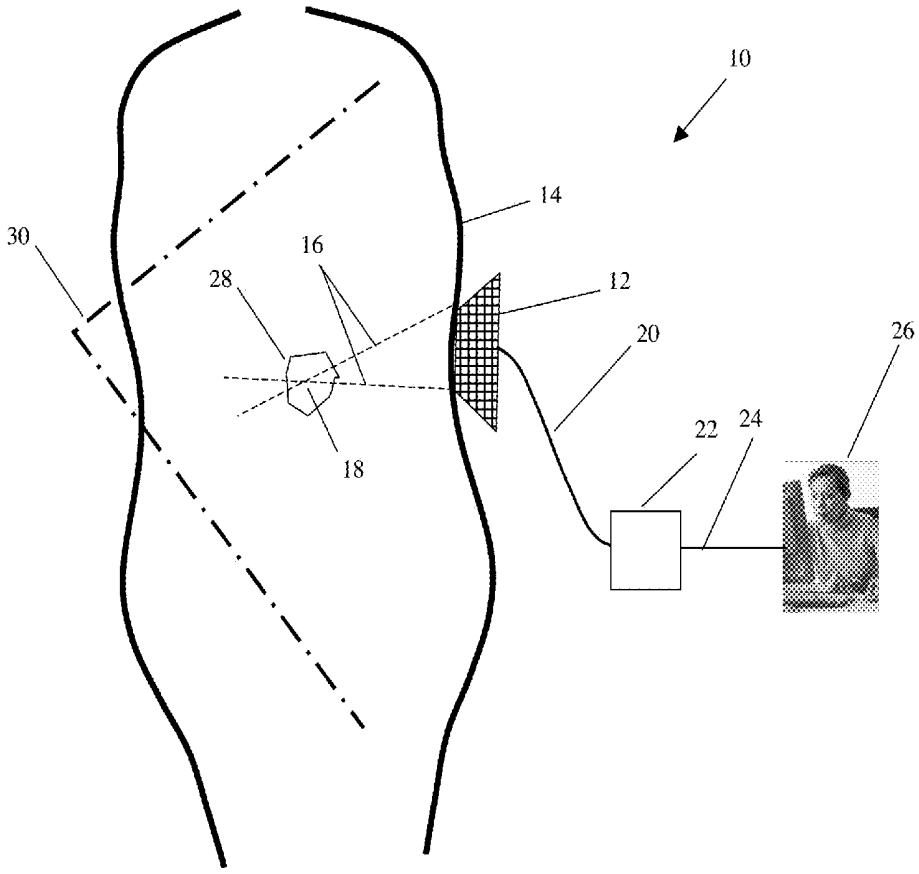

FIG 2
EXISTING ART

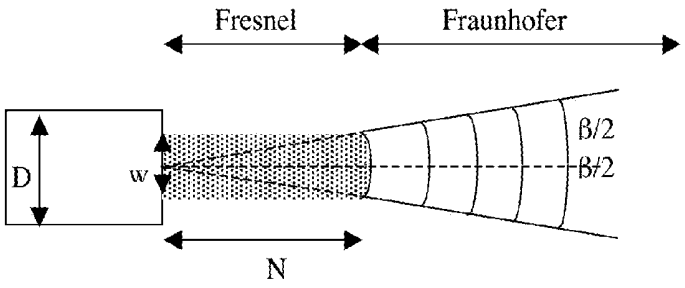

FIG 3a

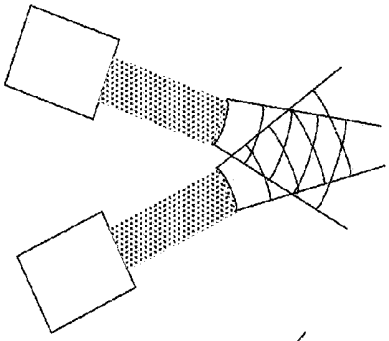

FIG 3b

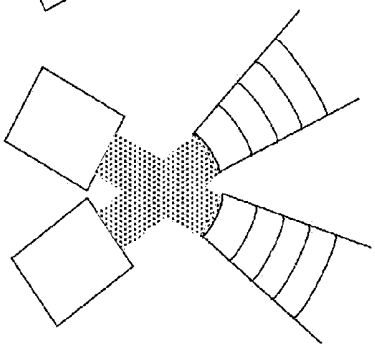

FIG 3c

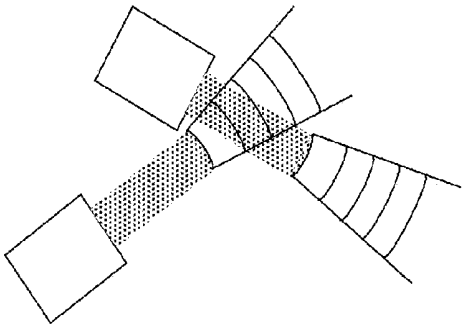

FIG 3d

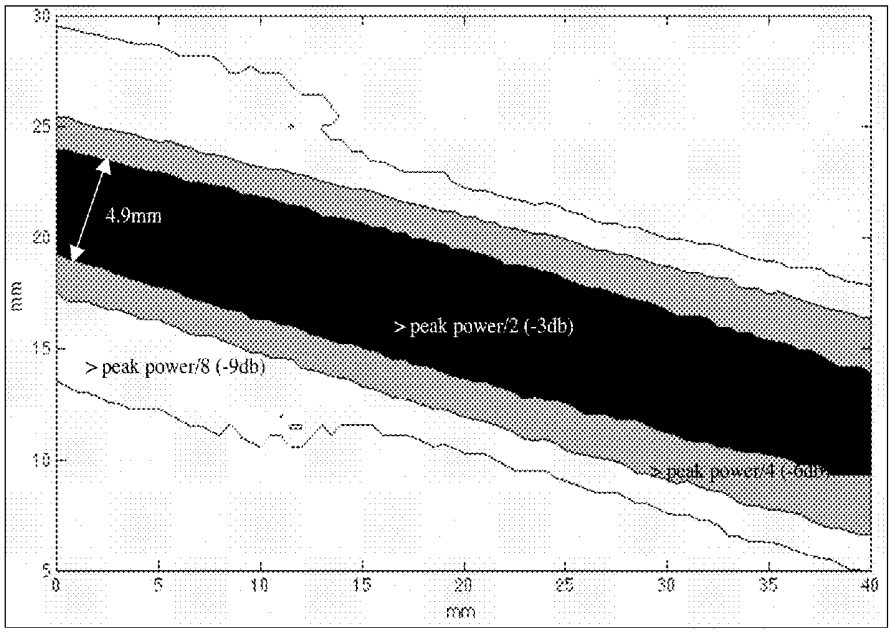
4.9mm
> peak power/2 (-3db)
> peak power/8 (-9db)
> peak power/4 (-6db)
mm
mm
0
5
10
15
20
25
30
35
40

FIG 4

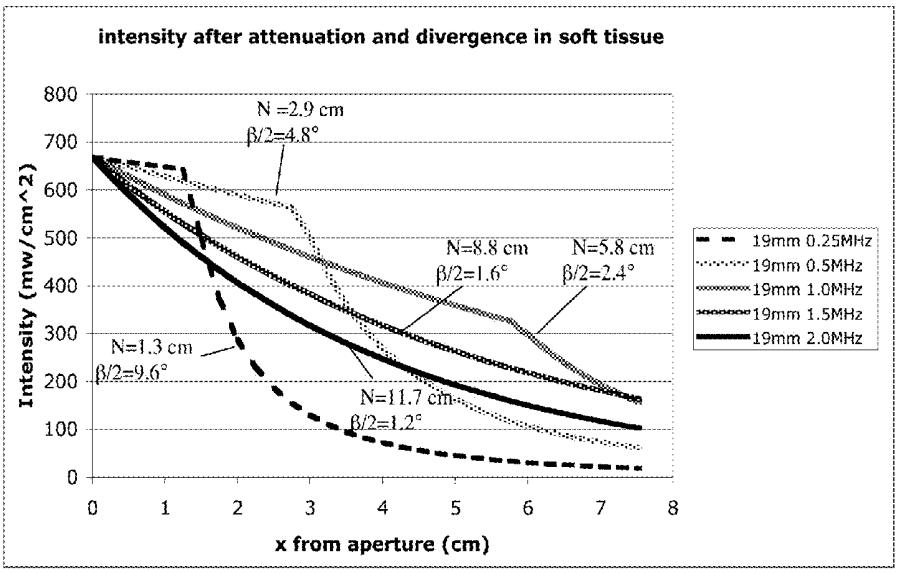
intensity after attenuation and divergence in soft tissue
Intensity (mw/cm^2)
x from aperture (cm)
N =2.9 cm
β/2=4.8°
N=8.8 cm
β/2=1.6°
N=5.8 cm
β/2=2.4°
N=1.3 cm
β/2=9.6°
N=11.7 cm
β/2=1.2°
19mm 0.25MHz
19mm 0.5MHz
19mm 1.0MHz
19mm 1.5MHz
19mm 2.0MHz

FIG 5

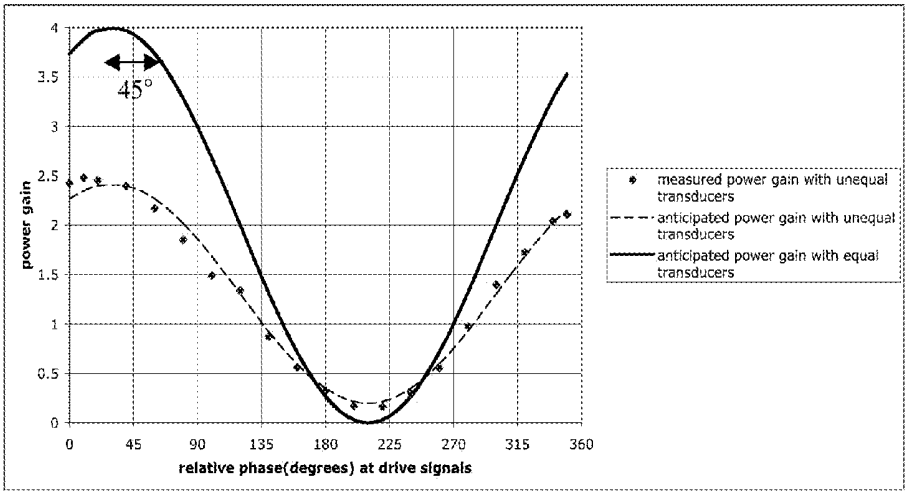
power gain
relative phase(degrees) at drive signals
45°
measured power gain with unequal transducers
anticipated power gain with unequal transducers
anticipated power gain with equal transducers

FIG 6

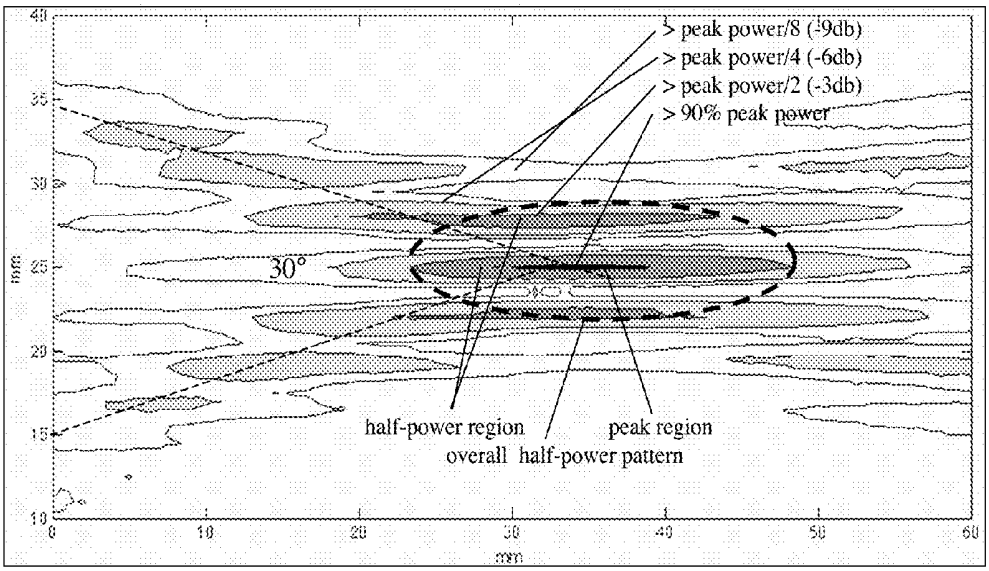
> peak power/8 (-9db)
> peak power/4 (-6db)
> peak power/2 (-3db)
> 90% peak power
30°
half-power region
peak region
overall half-power pattern
mm
mm

(a)

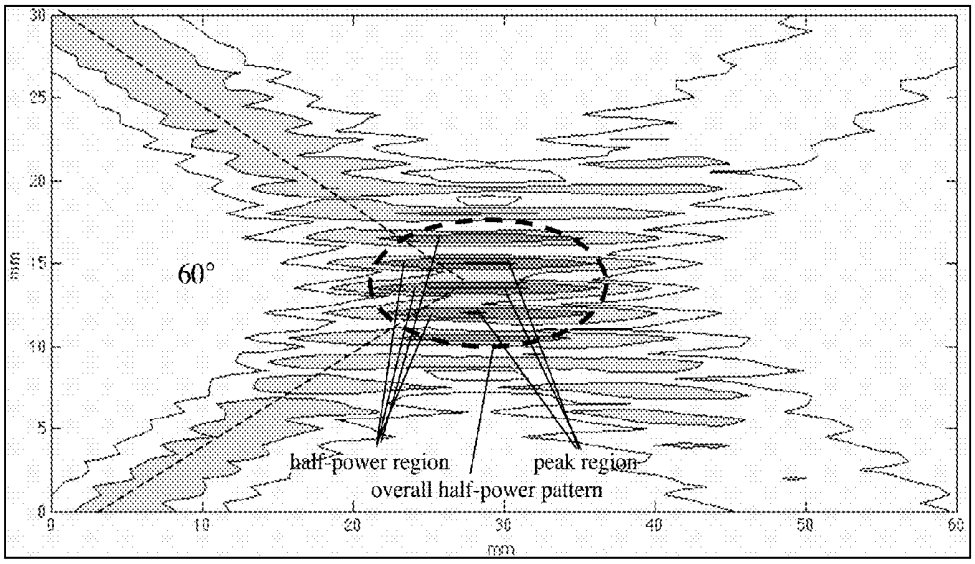
60°
half-power region
peak region
overall half-power pattern
mm
mm

(b)

FIG 7

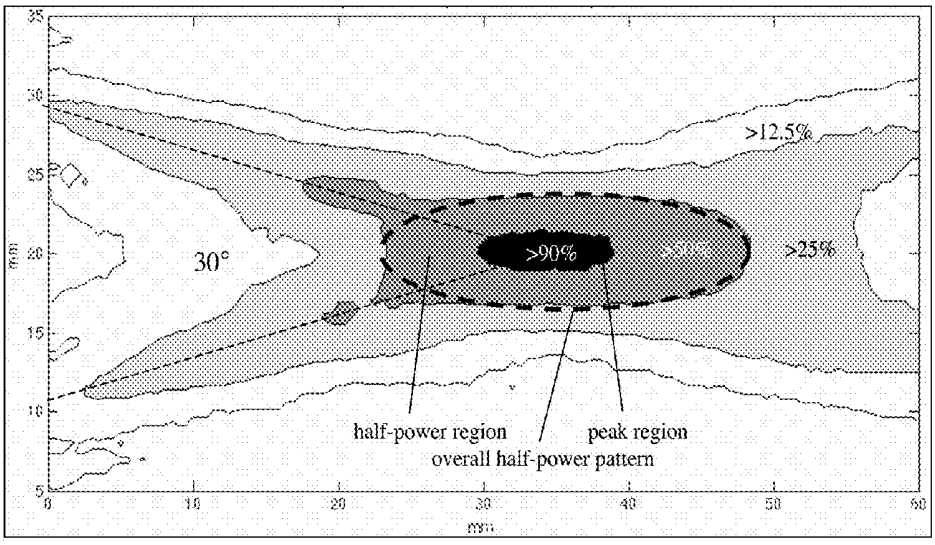
>12.5%
30°
>90%
>25%
half-power region
peak region
overall half-power pattern
mm
mm

FIG 8

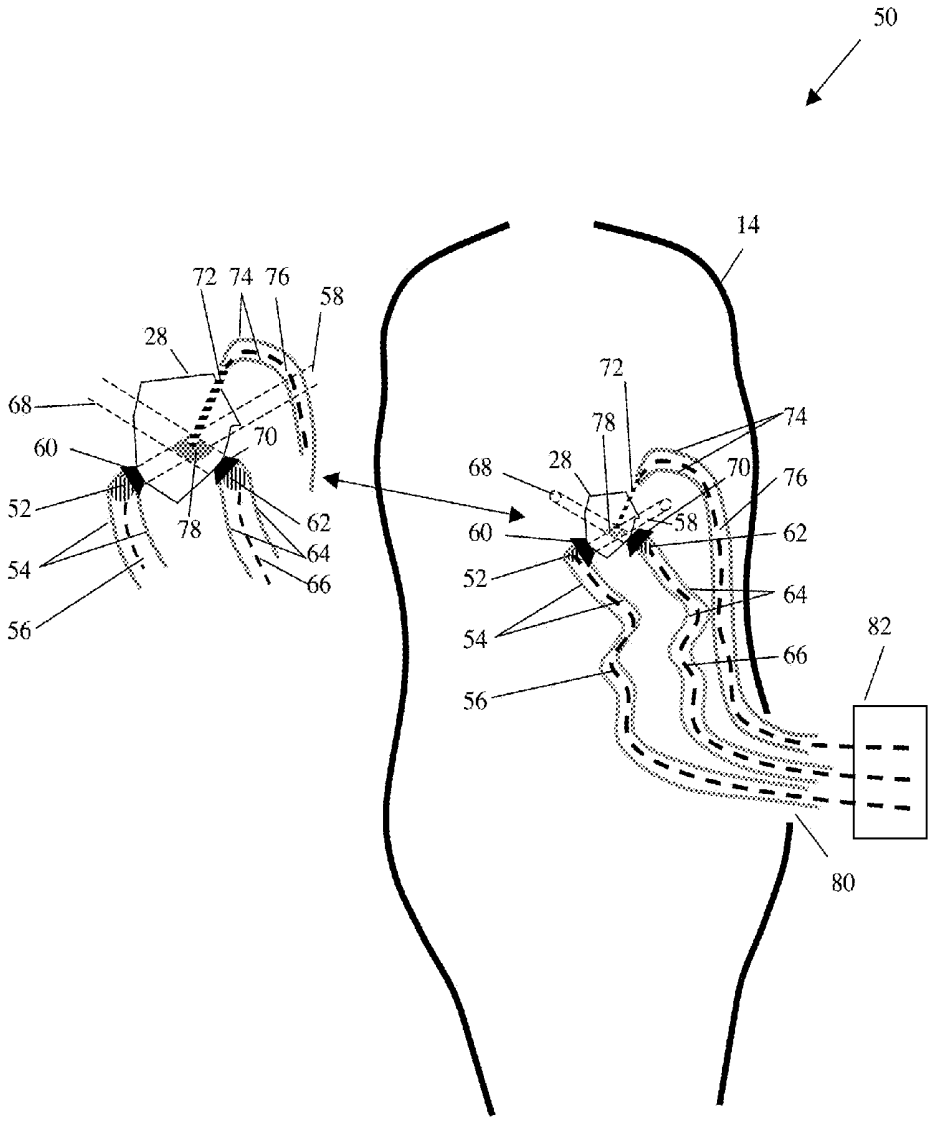
50
14
72
74
76
58
28
68
60
70
52
78
62
64
54
66
56
72
78
74
28
68
70
76
58
60
62
52
64
54
66
82
56
80

FIG 9

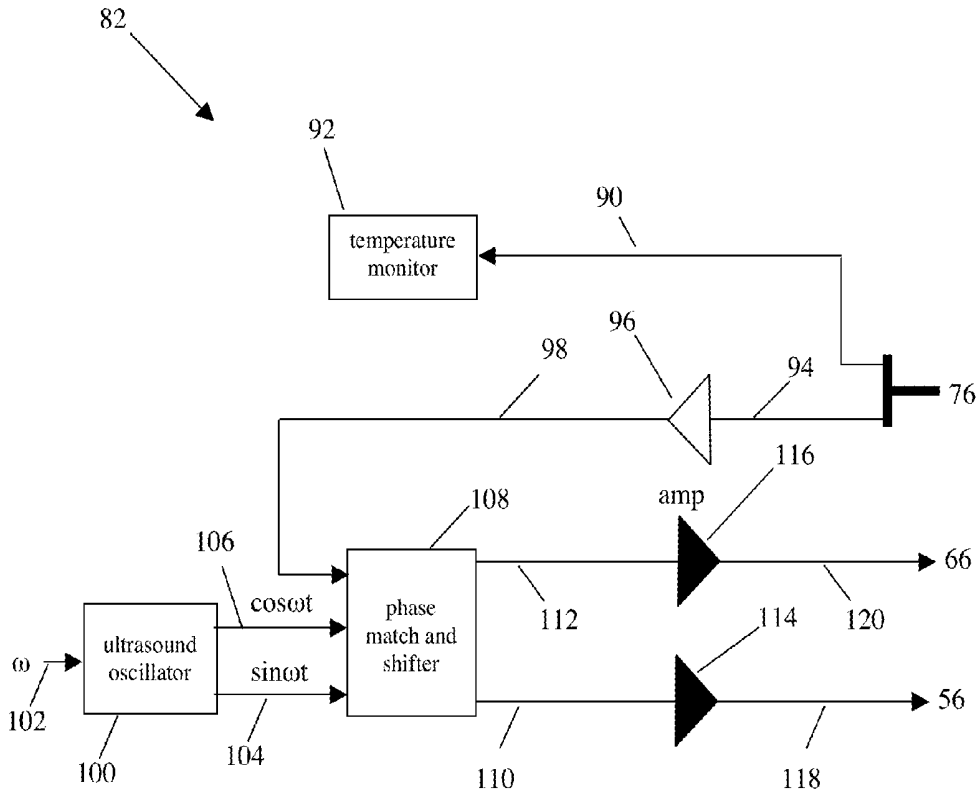
82
92
temperature monitor
90
96
98
94
76
116
amp
108
106
66
cosωt
phase match and shifter
112
114
120
ω
ultrasound oscillator
sinωt
56
102
100
104
110
118

FIG 10

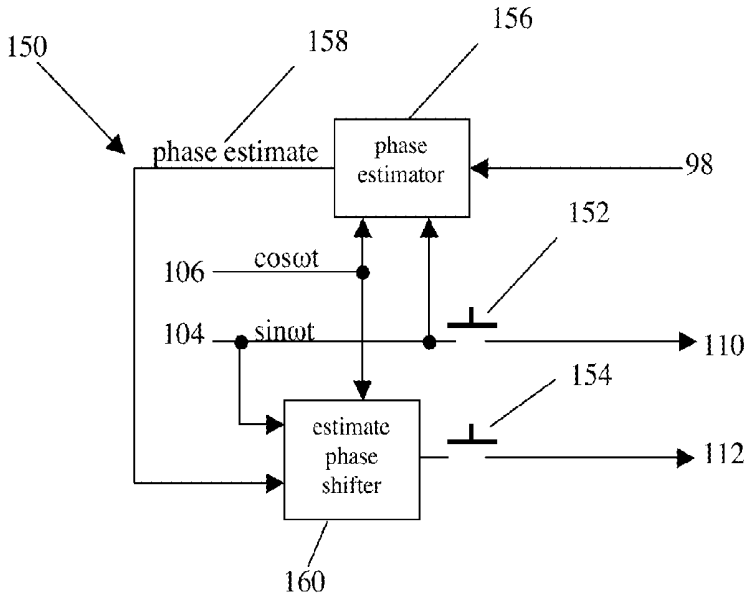
150
158
156
phase estimate
phase estimator
98
152
106
cosωt
104
sinωt
110
154
estimate phase shifter
112
160

FIG 11

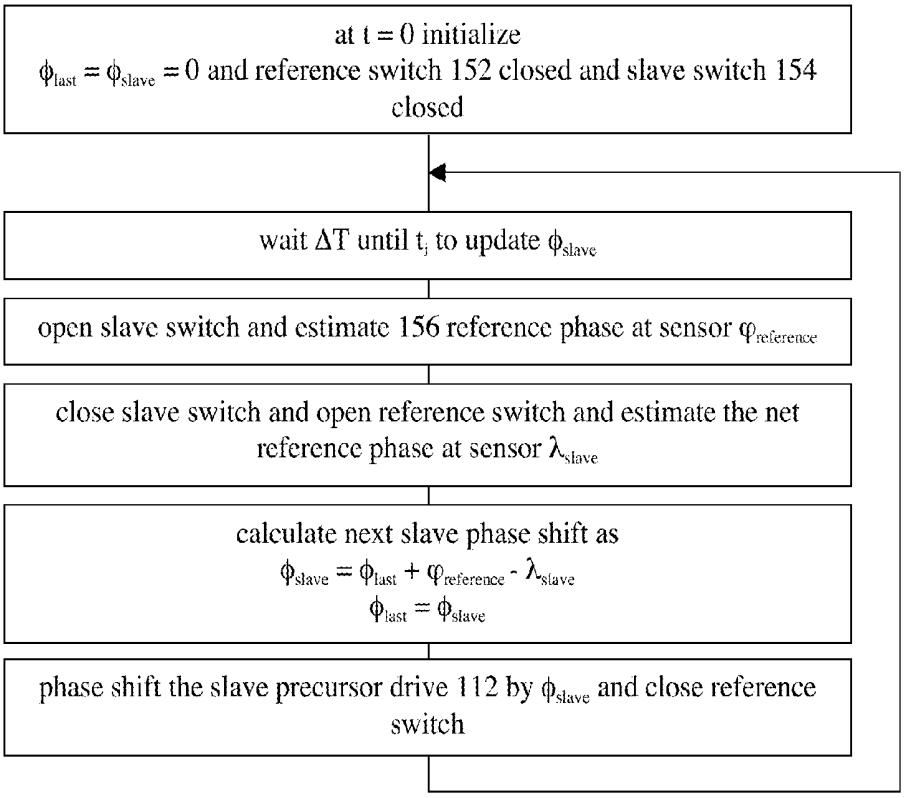
at t = 0 initialize
$\phi_{last} = \phi_{slave} = 0$ and reference switch 152 closed and slave switch 154 closed
wait ΔT until t_j to update ϕ_{slave}
open slave switch and estimate 156 reference phase at sensor $\varphi_{reference}$
close slave switch and open reference switch and estimate the net reference phase at sensor λ_{slave}
calculate next slave phase shift as
$\phi_{slave} = \phi_{last} + \varphi_{reference} - \lambda_{slave}$
$\phi_{last} = \phi_{slave}$
phase shift the slave precursor drive 112 by ϕ_{slave} and close reference switch

FIG 12

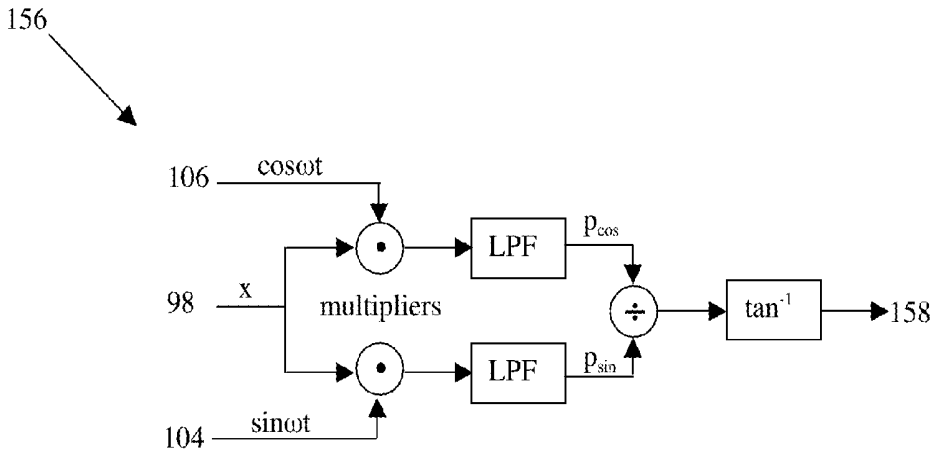
156
106
cosωt
98
x
multipliers
LPF
LPF
p_{cos}
p_{sin}
÷
tan^{-1}
158
104
sinωt

(a)

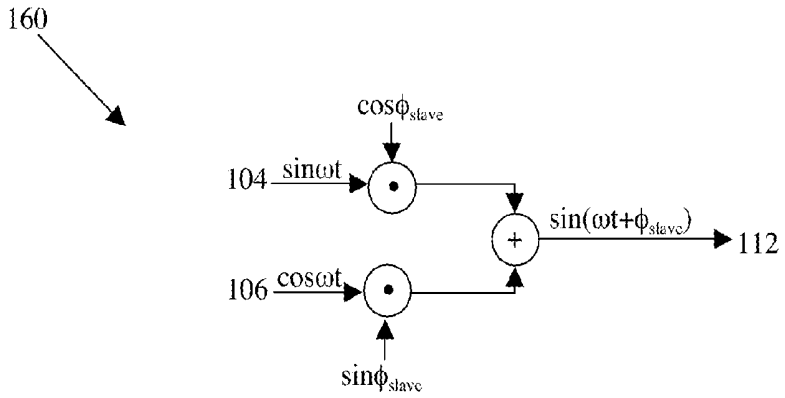
160
cosϕslave
104
sinωt
106
cosωt
sinϕslave
+
sin(ωt+ϕslave)
112

(b)

FIG 13

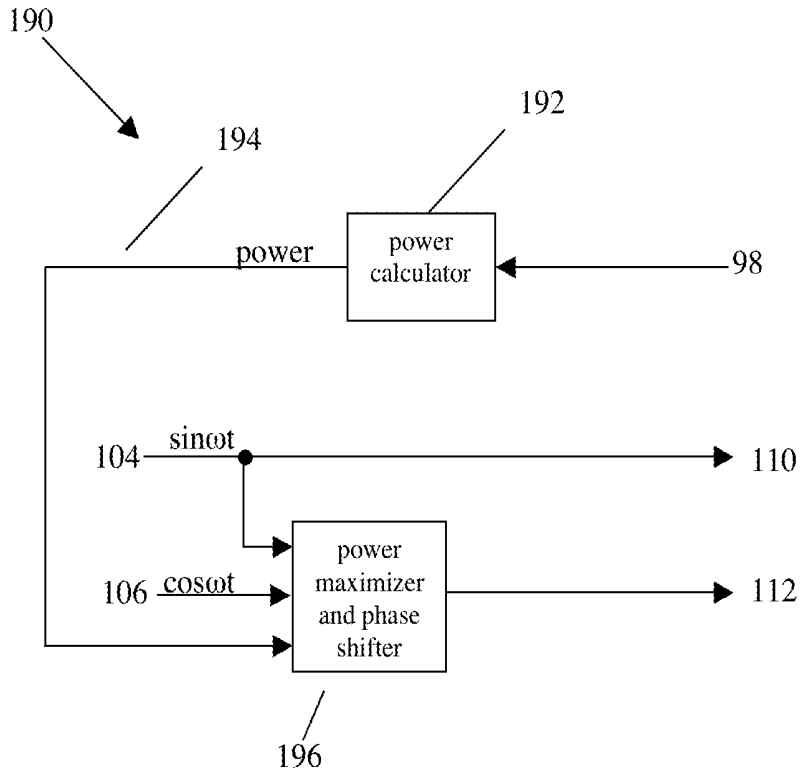
190
192
194
power
power calculator
98
104
sinωt
110
power maximizer and phase shifter
106
cosωt
112
196

FIG 14

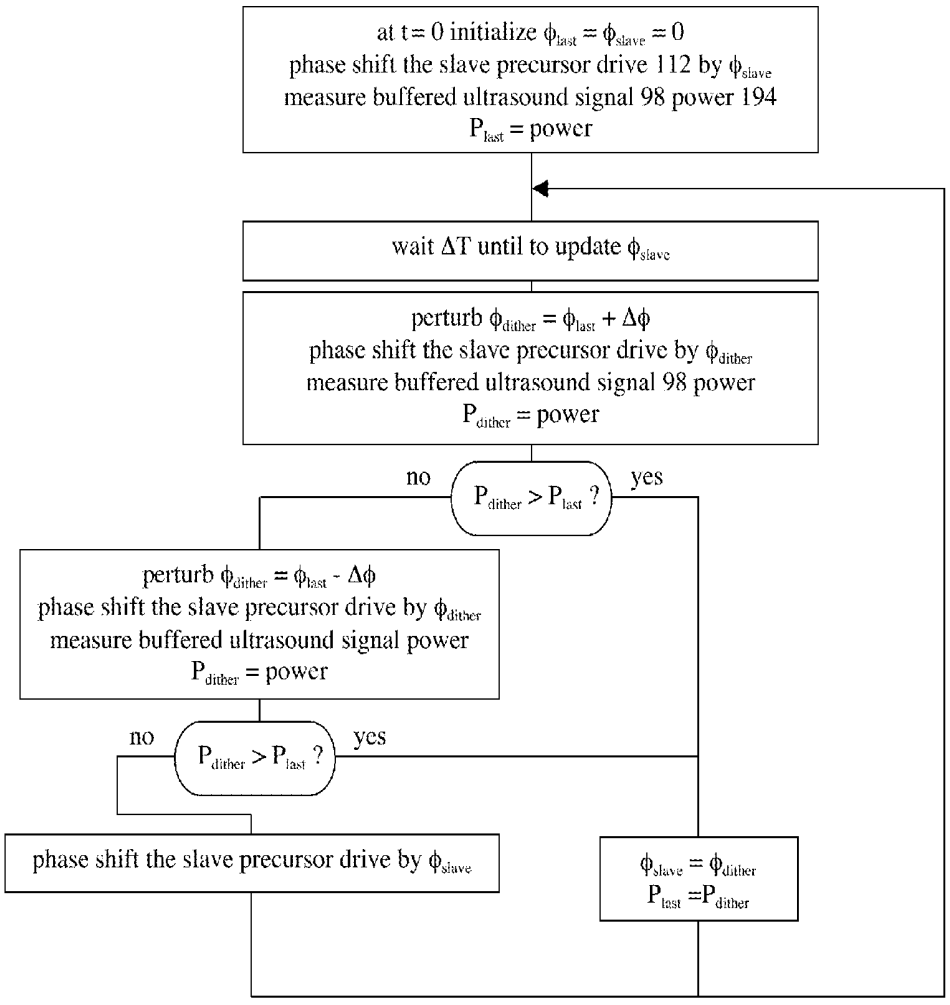
at t = 0 initialize $\phi_{last} = \phi_{slave} = 0$
phase shift the slave precursor drive 112 by ϕ_{slave}
measure buffered ultrasound signal 98 power 194
P_{last} = power
wait ΔT until to update ϕ_{slave}
perturb $\phi_{dither} = \phi_{last} + \Delta\phi$
phase shift the slave precursor drive by ϕ_{dither}
measure buffered ultrasound signal 98 power
P_{dither} = power
no
$P_{dither} > P_{last}$?
yes
perturb $\phi_{dither} = \phi_{last} - \Delta\phi$
phase shift the slave precursor drive by ϕ_{dither}
measure buffered ultrasound signal power
P_{dither} = power
no
$P_{dither} > P_{last}$?
yes
phase shift the slave precursor drive by ϕ_{slave}
$\phi_{slave} = \phi_{dither}$
$P_{last} = P_{dither}$

FIG 15

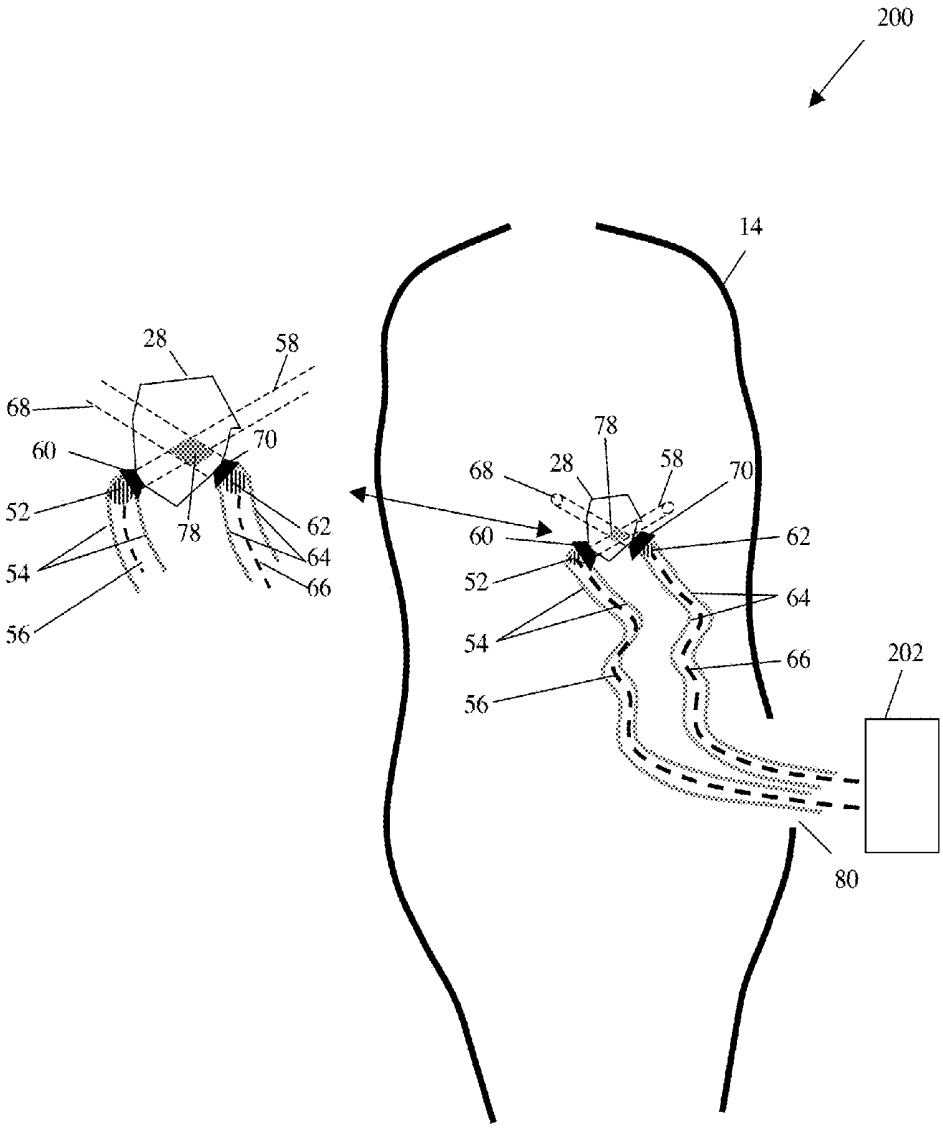

FIG 16

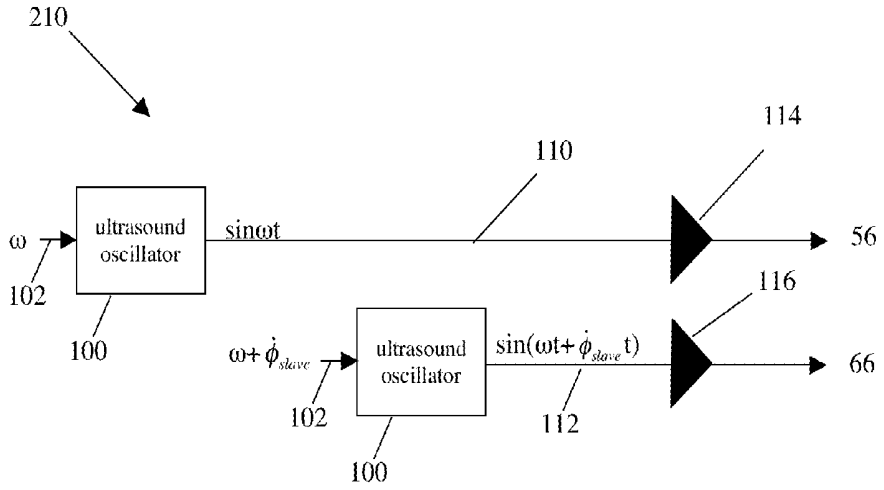
210
114
110
ω
ultrasound oscillator
sinωt
56
102
100
116
ω+ $\dot{\phi}_{slave}$
ultrasound oscillator
sin(ωt+ $\dot{\phi}_{slave}$ t)
66
102
112
100

FIG 17

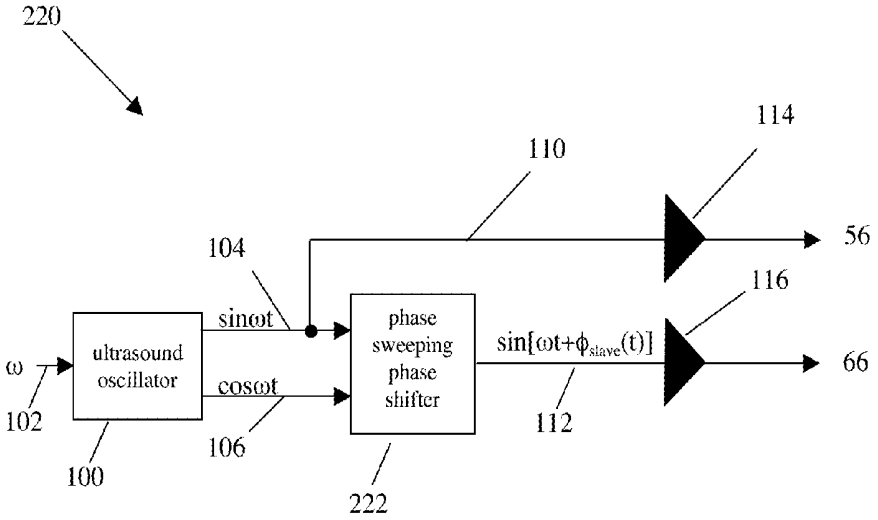
220
114
110
104
56
116
ω
ultrasound oscillator
sinωt
phase sweeping phase shifter
sin[ωt+ϕ_{slave}(t)]
66
cosωt
102
112
106
100
222

FIG 18

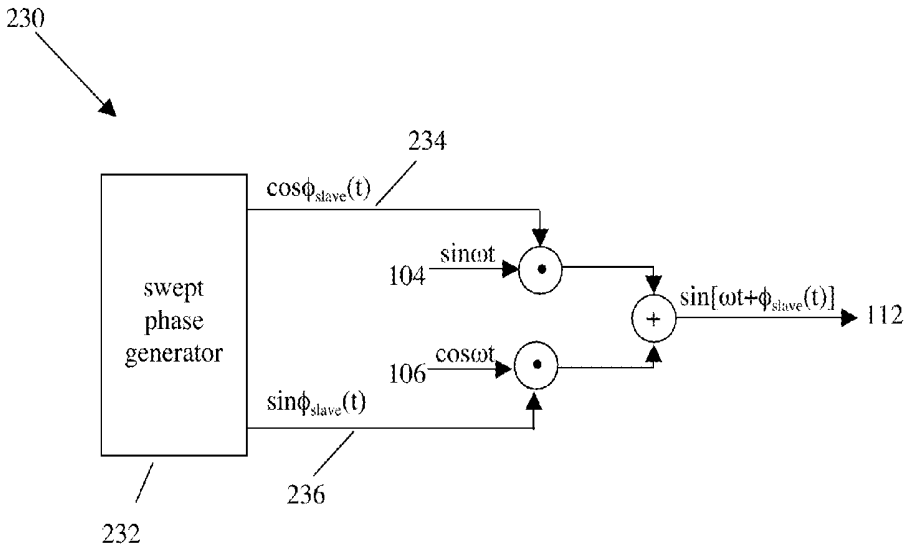
230
234
cosϕslave(t)
swept
phase
generator
sinωt
104
sin[ωt+ϕslave(t)]
112
+
cosωt
106
sinϕslave(t)
236
232

FIG 19

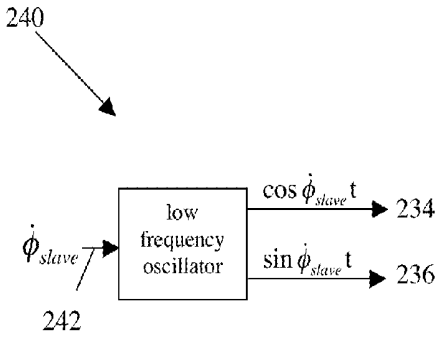
240
low
frequency
oscillator
cos ϕ̇slave t
234
sin ϕ̇slave t
236
ϕ̇slave
242

FIG 20

MULTI-BEAM ULTRASOUND DEVICE

RELATED APPLICATIONS

[0001] This application claims the benefit of U.S. Provisional Application Ser. No. 61/725,351 filed 12 Nov. 2012.

BACKGROUND OF THE INVENTION

[0002] 1. Field of the Invention

[0003] The invention relates generally to devices for applying ultrasound directed energy. More particularly, the present invention relates to apparatus and methods to apply ultrasound for medical therapy.

[0004] 2. General Background and State of the Art

[0005] Surgical intervention has long been the standard of care to correct physical tissue defects including tumors, atrial fibrillation, and arteriosclerosis. Minimally invasive endoscopic or laparoscopic surgery has been introduced to minimize trauma and speed recovery. In an effort to avoid surgery entirely and to provide care where surgery is impossible, directed ionizing radiation beams, such as X-ray, have been developed to affect tissue remotely by damaging the DNA and causing tissue death by halting the production of proteins required for life.

[0006] Ultrasound is another form of directed energy that avoids the significant side affects and risks of ionizing radiation. Ultrasound affects tissue by propagating an acoustic pressure wave, and this wave causes slight vibration of the tissue in its path. The tissue resistance to vibration generates heat, and the sufficiently prolonged application of heat causes temperature rise and cellular death by denaturizing proteins and enzymes required for life, and by cavitation. Denaturation is where the shape of a biological molecule is altered such that it loses its biologic function, and cavitation is the creation of gas bubbles that implode and cause general tissue damage. As in the case of ionizing energy beams, efforts must be made to avoid damage to healthy tissue surrounding the target tissue.

[0007] High Intensity Focused Ultrasound (HIFU) is the current state of the art. HIFU emits a focused acoustic beam that, initially wide, focuses down to a small volume at the target tissue. Away from the focus the beam intensity is low so as not to damage healthy tissue while the intensity at the ellipsoidal (1 mm by 10 mm-5 mm^3) focus does damage. The small incremental ellipsoid is scanned through the target tissue by moving the beam. HIFU is used in conjunction with a Magnetic Resonance Imaging (MRI), an imaging device that also senses heat, to verify the location of the focus before full power is applied. Even with MRI, the Federal Drug Administration (FDA) only sanctions use of HIFU for uterine fibroid tumors where there is low risk of scattering the high intensity onto healthy tissue by bone and gas pockets. To minimize inadvertent scattering, the patient is fully anesthetized during the 3-5 hour fibroid procedure while prone within the MRI.

[0008] There is a need to have a means to introduce surgically effective ultrasound that is safer than HIFU, can be applied more widely than to uterine fibroids, and does not require an expensive MRI watchdog device. It is further advantageous to treat an incremental volume greater than the 5 mm^3 HIFU focus.

BRIEF SUMMARY OF THE INVENTION

[0009] The fundamental concept behind this invention is this use of at least two ultrasound transducers with each having an acoustic beam with intensity too low to affect tissue, but arranged to intersect at the target volume with controlled relative phase. The controlled phase adjusts the beam interference such that the resultant is a merged beam of greater intensity, no longer benign, that can affect the targeted tissue and not surrounding tissue.

[0010] The object of the invention is to provide a therapeutically effective ultrasound device that can go where HIFU cannot, is safer, is less expensive, does not require an MRI, and handles larger incremental volumes. Further objects and advantages of the present invention will become more apparent from the following description of the preferred embodiments which, taken in conjunction with the accompanying drawings, illustrate, by way of example, the principles of the invention.

DESCRIPTION OF THE DRAWINGS

[0011] FIG. **1** is a graphical depiction of the approximate time cellular temperature must be held for cellular death by denaturation.

[0012] FIG. **2** is a schematic representation of existing art HIFU therapeutic ultrasound.

[0013] FIG. **3** is a schematic representation of (a) an ultrasound beam from an unfocused transducer and (b-d) the three ways two such beams can intersect.

[0014] FIG. **4** is a graphical display of measurements of the power delivered by a single 1 MHz 19 mm unfocused ultrasound transducer showing the contours of the −3 db, −6 db and −9 db peak power regions.

[0015] FIG. **5** is a graphical representation of the calculated intensity delivered by a single 19 mm unfocused transducer in soft tissue operated at 0.25, 0.50, 1.0, 1.5, and 2.0 MHz and illustrating the effect of frequency and distance on attenuation and beam divergence.

[0016] FIG. **6** is a graphical representation of the calculated and measured power gain, as a function of relative phase at the drivers, of a point within the intersection of two unequal 40 MHz transducers in water, and the projected power gain had they been equal.

[0017] FIG. **7** (*a*) is a graphical display of power from measurements of two 30° intersecting ultrasound beams from two equal 1 MHz 19 mm unfocused transducers with fixed phase and showing the contours of the 90%, −3 db, −6 db and −9 db peak power regions; (b) is a graphical display of power from measurements of two 60° intersecting ultrasound beams from two equal 1 MHz 19 mm unfocused transducers with fixed phase and showing the contours of the 90%, −3 db, −6 db and −9 db peak power regions.

[0018] FIG. **8** is a graphical display of power from measurements of two 30° intersecting ultrasound beams from two equal 1 MHz 19 mm unfocused transducers with swept phase and showing the contours of the 90%, −3 db (50%), −6 db (25%) and −9 db (12.5%) peak power regions.

[0019] FIG. **9** is a schematic representation of intersecting transducers using match phase approach.

[0020] FIG. **10** is a schematic representation of a phase matching drive generator.

[0021] FIG. **11** is a schematic representation of a phase match and shifter having phase estimating capability.

[0022] FIG. **12** is a flowchart of an algorithm for controlling phase using the phase match and shifter having phase estimating capability.

[0023] FIG. **13** is (a) a schematic representation of an analog embodiment of the phase estimator; (b) a schematic representation of analog embodiment of the estimate phase shifter.

[0024] FIG. **14** is a schematic representation of a phase match and shifter having power maximizing capability.

[0025] FIG. **15** is a flowchart of an algorithm to estimate phase by maximizing power.

[0026] FIG. **16** is a schematic representation of intersecting transducers using swept phase approach.

[0027] FIG. **17** is a schematic representation of a phase sweeping drive generator using two ultrasound oscillators.

[0028] FIG. **18** is a schematic representation of a phase sweeping drive generator using a single ultrasound oscillator.

[0029] FIG. **19** is a schematic representation of a phase sweeping phase shifter.

[0030] FIG. **20** is a schematic representing a swept phase generator using a low frequency oscillator.

EXISTING ART

[0031] The common purpose of ultrasound application is to warm the tissue sufficiently and for a sufficient time to cause death. As a rule-of-thumb, this combination of tissue temperature and application time begins with the minimal combination of 43° C. for 120 minutes, with the duration falling by half with each 1° C. rise thereafter as illustrated in FIG. **1**. Another purpose would be to trigger cavitation implosions, but these are difficult to control and less commonly used.

[0032] FIG. **2** illustrates a conventional HIFU surgical ultrasound device **10** having an ultrasound HIFU transducer **12** mounted external to the patient surface **14** (typically skin). The transducer emits a conical ultrasound beam **16** with a high intensity focal point **18**, and is coupled through an electrical cable **20** to the drive generator and beam direction electronics **22**. An operator-computer combination **26**, connected to the signal generator and beam direction electronics by a cable **24**, controls the operation of the device in order to scan the target volume **28** in small incremental volumes. The manner in which the beam is generated includes having a phased array transducer where the beam shape and direction is selected by judicious phased activation of many small transducers, or by having a single transducer shaped as a portion of a sphere with direction selected by mechanical actuators.

[0033] In operation, the operator-computer **26** directs the HIFU beam **16** to form a focus **18** within the target volume **28** at low power and at a desired spot, and an MRI device **30** is operated to scan the patient and image the spot warmed by the low power beam to verify the actual anatomical location of the spot. If the operator-computer determines the focus is located as desired, the HIFU transducer **12** is operated at high power to damage the tissue. This procedure is repeated many times to cover the target volume in small ellipsoidal volume increments of approximately 5 mm^3.

Technical Background and Experimental Results

General Concept

[0034] Ultrasound beams are traveling waves of acoustic pressure produced by ultrasonic transducers. As waves, they interact with other acoustic waves with classical interference patterns having repeating constructive and destructive interference. Destructive interference occurs when traveling waves are out of phase and partially or fully cancel each other, and constructive interference is when the waves are in phase and build on each other. It is possible, using phase control, to modify the interference pattern and apply acoustic beams with low intensities that do not affect surrounding tissue yet have greater therapeutic intensity at their intersection. The invention is to emit a plurality of intersecting ultrasound beams while controlling their phasing such that the resulting intersection at the target tissue takes advantage of interference.

[0035] A Single Beam:

[0036] FIG. **3***a* illustrates a single unfocused transducer having aperture diameter D and designed to generate an unfocused acoustic beam of frequency f into a medium having speed of sound s and acoustic signal attenuation α. As illustrated in FIG. **3***a* and defined in TBL 1, an unfocused circular transducer produces an acoustic beam having initial nominal width w that diverges with angle β resulting in its energy being dispersed over an increasingly wider area. The beam is stable but poorly defined until the Far Field Fraunhofer region beyond the Near Field Fresnel Zone. Within the Near Field Fresnel zone the beam is essentially cylindrical and interferes with itself as it radiates from multiple points on the vibrating transducer active surface, and the region has multiple interference maxima and minima. Within the Far Field Fraunhofer zone the beam ceases to interfere with itself and becomes an expanding (as per the divergence angle) and well-defined pressure wave. The Near Field distance N is that of the last Fresnel interference maxima and defines the transition from Fresnel to Fraunhofer zones.

[0037] TBL 2 presents s and a for various tissues along with, at two frequencies, the calculated wavelength λ and distance to half-power (−3 db) due to attenuation by tissue and scattering. Using soft tissue as the typical target, 1 MHz and 10 MHz beams have, respectively, λ of 0.154 cm and 0.015 cm and have lost half their power after 5.6 cm and 0.56 cm. The frequency of therapeutic ultrasound is typically chosen around 1 MHz to reduce attenuation.

[0038] TBL 3 illustrates the effect of various aperture diameters on width w, Near Field distance N and divergence angle β of a 1 MHz unfocused transducer in soft tissue. The tubular enclosure column shows the catheter type or laparoscopy trocar having the same diameter as the transducer.

[0039] FIG. **4** is a two-dimensional contour plot of the measured peak power along the main axis of a 1 MHz 19 mm diameter unfocused transducer (Olympus A314S-SU) operating in a water bath. Its characteristics are shown in TBL 3 in agreement with FIG. **4**.

[0040] Therapeutically, the power intensity I (watts/cm^2) is the power density applied to tissues. The beam radius along the axis is, essentially, constant in the Fresnel zone but increases in the Fraunhofer zone as the beam diverges after the near field distance N. Tissue attenuation of the signal occurs throughout its path, and the beam intensity is modeled as

$$\text{attenuation: } P = P_0 10^{-f\alpha x/10}$$

$$\text{beam radius: } r = \begin{cases} r_0 & \text{for } x < N \\ r_0 + (x - N)\tan(\beta/2) & \text{for } x \geq N \end{cases}$$

$$\text{beam area: } A = \pi r^2$$

$$\text{beam intensity: } I = \frac{P}{A}$$

where P_0 is the transducer power output, r_0 is the radius (half-width) of the beam at the aperture, and x is the distance from the aperture. Including the equations of TBL 1, FIG. **5** illustrates the intensity of a 125 mW 19 mm unfocused transducer in soft tissue. Initial Fresnel zone interaction is only attenuation, and the following Fraunhofer zone interactions are attenuation and dispersion due to angular divergence angle β. The lower the transducer frequency, the shorter the Fresnel zone, the greater the dispersion, and the shallower the therapeutic affect.

[0041] Scattering:

[0042] One challenge ultrasound has is the direction change due to scattering by non-homogenous tissues. Scattering is a general term describing the change of the sound direction of travel due to interaction with non-homogenous tissues, and is a component of acoustic attenuation by tissue. At the boundary between different tissues, having different acoustic impedance and speed of sound, the wavelike properties of sound cause transmission and reflection. If γ_0 is the angle between an incident beam and the vertical to the boundary and s_0 is the incident speed of sound, Snell's Law defines the corresponding angles of the reflected and transmitted portions according to

$$\gamma_{reflected} = \gamma_0$$

$$\gamma_{transmitted} = \sin^{-1}\left(\frac{s_1}{s_0}\sin\gamma_0\right)$$

The angle of the transmitted wave is not the same as the incident meaning the transmitted wave is moving in a different direction. The quantity reflected is dependent on the acoustic impedances of the tissue on each side of the boundary with an Intensity Reflection Coefficient given by

$$IRC = \frac{\text{reflected intensity } (W/\text{cm}^2)}{\text{incident intensity } (W/\text{cm}^2)} = \left(\frac{Z_1 - Z_0}{Z_1 + Z_0}\right)^2$$

where Z_0 is the acoustic impedance of the source side of the boundary, and Z_1 is that of the transmitted side. Air (contents of the intestine, stomach, lungs) and bone have dramatically different impedance than tissue and will strongly reflect sound.

[0043] Intersection of Two Beams:

[0044] FIGS. **3***b*, **3***c* and **3***d* illustrate three types of intersections: FIG. **3***b* Fraunhofer-Fraunhofer, FIG. **3***c* Fresnel-Fresnel, and FIG. **3***d* Fresnel-Fraunhofer. All three types form standing interference patterns given continuous sinusoidal excitation. Given a relative phase ϕ, at a point in the intersection, a sinusoidal pressure wave from a first transducer beam $a_{first}\sin(\omega t)$ and a sinusoidal pressure wave from a second transducer beam $a_{second}\sin(\omega t+\phi)$ combine by superposition and sum to form a resultant sinusoidal pressure wave with amplitude given by the well known sum-of-sines-with-equal-frequency equation

$$a_{resultant} = \sqrt{a^2_{first} + a^2_{second} + 2a_{first}a_{second}\cos\phi}$$

The peak power in the resultant is proportional to the square of the amplitude:

$$P_{resultant} \propto a^2_{first} + a^2_{second} + 2a_{first}a_{second}\cos\phi \quad (1)$$

Compared to the peak power of the first transducer, the peak power gain is

$$G_P = \frac{a^2_{first} + a^2_{second} + 2a_{first}a_{second}\cos\phi}{a^2_{first}} = 1 + \frac{a^2_{second} + 2a_{first}a_{second}\cos\phi}{a^2_{first}} = 1 + \frac{a^2_{second}}{a^2_{first}} + \frac{2a_{second}}{a_{first}}\cos\phi \quad (2)$$

If $a_{first}=a_{second}$ then

$$G_P = 2(1+\cos\phi)$$

and the power gain is maximum 4× when ϕ=0 and minimum 0× when ϕ=π. FIG. **6** shows tight agreement between the measured and expected power gain G_P, from Eq. 2, for two intersecting 40 MHz transducers in water with various phase values, and measured by a fixed hydrophone. The hydrophone measured the signals generated by the two transducers, one at a time, as having amplitudes: a_{first}=8.56 mV and a_{second}=4.74 mV. The phase values are set at the transducer drive sources, and not at the intersection where the hydrophone was fixed, and thus have a 35° offset due to electronics and relative transducer positions from the hydrophone. Also shown is the equivalent power curve should $a_{first}=a_{second}$ illustrating the anticipated 0× min and 4× max values.

[0045] FIG. **6** shows the maximum power point is not greatly sensitive to phase: 90% of the peak power is contained within ±45° of the optimum phase.

[0046] Fixed Phase Intersections:

[0047] FIG. **7***a* presents the measured power contours from two Fraunhofer-Fraunhofer intersecting beams (FIG. **3***b*) in water from identical 1 MHz 19 mm transducers of FIG. **4** with a 30° angle between them. The transducers have had their drive signals phased so as to produce a fixed matched-phase peak at the center of image. Several islands of peaks and valleys are seen, and the small (less than 1 mm×10 mm) black 90% peak power region has power gain 4× that of the arriving beams (light gray). The dual 4.8 mm wide beams produce several half-power regions (dark gray), and an ellipsoidal overall half-power pattern that is around 7 mm×25 mm (641 mm^3).

[0048] FIG. **7***b* shows the measured power contours of 60° angular intersection in water and having a larger number of islands of peaks and valleys with a shorter ellipsoidal overall half-power pattern of around 7 mm×17 mm. As the intersection angle approaches 90°, the overall pattern is expected to approach spherical with nearly a 7 mm diameter (179 mm^3).

[0049] Swept Phase Intersections:

[0050] Changing the relative phase of the intersecting beams moves the interference patterns but not the overall half-power pattern. FIG. **8** presents the measured power contours from two Fraunhofer-Fraunhofer intersecting beams in water from identical 1 MHz 19 mm transducers of FIG. **4** having a 30° angle between them, and where the transducers have their relative phase of their drive signals continuously and linearly swept from 0° to 360°. The islands of peaks and valleys are eliminated, and the peak region is 2.5 mm×10 mm and remains 4× that of the arriving beams. The 4.8 mm beams produce an overall half-power pattern that is 7 mm×25 mm, the same as for FIG. **6** of the fixed phase intersection.

[0051] Linear sweeping of phase means $\phi(t)=\dot{\phi}t$ where

$$\dot{\phi} = \frac{d}{dt}\phi(t)$$

is the phase sweep rate. The swept drive signal is then

$$\sin[\omega t+\phi(t)]=\sin[\omega t+\dot{\phi}t] \quad (3)$$

$$\sin[\omega t+\phi(t)]=\sin[\omega+\dot{\phi}t] \quad (4)$$

This establishes that a swept phase angle is produced by drive signals with differing frequencies where the difference is the phase sweep rate.

DETAILED DESCRIPTION OF PREFERRED EMBODIMENT

[0052] Based on the experimental and theoretical considerations presented in the Technical Background and Experimental Results section, two among many approaches to operate intersecting ultrasound transducers are here described. Both approaches produce a 4× power gain at the beam intersection compared to surrounding tissue.

[0053] The first approach is a matched phase approach where the beams at the intersection are made to have essentially equal phase to take advantage of constructive interference, and this approach is shown to have at least two implementations: one that estimates the individual transducer phases at the target site and directly constructs a phase match, and a second that maximizes the measured power delivered to the target site and indirectly constructs a phase match.

[0054] The second approach to operate intersecting ultrasound transducers is a swept phase implementation that smoothes the interference peaks and valleys and mitigates the wave cancellation interference pattern.

Intersecting Transducers Using Matched Phase Approach

[0055] Ultrasound energy does not have a particle equivalence; it has only wave properties, and waves interact with each other, canceling and summing depending on their relative phase locally at the target. Wave summation is taken advantage of by using intersecting ultrasound beams having identical frequency and phase matched at the target tissue, as in FIG. **7***a-b*. Small (1 mm×10 mm, similar to HIFU) high intensity areas (>90%) are produced with a power gain of 4× relative to tissue in the non-intersecting regions. Fraunhofer-Fraunhofer intersections are preferred where the intersecting beams are well defined, as in FIG. **3***b*. This implementation requires an ultrasonic sensor at or near the intersection of the transducer beams to report the transducer ultrasound signals, and the sensor may be configured to include a temperature probe to monitor therapy as per FIG. **1**.

[0056] The locations of the transducers and sensor are arranged directly by the medical professional performing the ultrasound therapy using manual, minimally invasive, or other means. Unlike HIFU, the transducers are very close, or proximal, to the target tissue.

[0057] FIG. **9** illustrates the intersecting transducers using matched phase approach **50**. A reference ultrasound transducer **52**, a slave ultrasound transducer **62**, and a sensor **72** responsive to ultrasonic pressure, and optionally including temperature sensing capabilities, are introduced through the patient surface **14** using minimally invasive surgical methods through portal **80** in order to treat an internal target tissue volume **28**. The sensor is preferably placed within the intersection **78**, and the reference transducer beam **58** is made to intersect with the slave transducer beam **68** in preferably a Fraunhofer-Fraunhofer manner. If the minimally invasive technique includes CO_2 to expand the region for surgical access, as in laparoscopy, the transducers include a reference couplant **60** and a slave couplant **70** to impedance match and route the ultrasound to the tissue through the gas. As needed, the reference transducer, slave transducer, and sensor are introduced through a reference tube **54**, a slave tube **64**, and a sensor tube **74** which may be distinct or combined. The transducers and sensor are connected to a phase matching drive generator **82** using reference cable **56**, slave cable **66**, and sensor cable **76**.

[0058] As illustrated in FIG. **10** of the phase matching drive generator **82**, the sensor **72** temperature signal **90**, if any, is delivered over sensor cable **76** and is used to monitor **92** the progress of therapy. The sensor ultrasound signal **94** is buffered by preamp **96** resulting in the buffered ultrasound signal **98**. An ultrasound oscillator **100** using frequency **102** produces sine **104** and cosine **106** (sine signal **104** phase shifted by 90°) signals that, along with the buffered ultrasound signal, are used by the phase match and shifter **108** to generate a precursor reference drive signal **110** and a precursor slave drive signal **112**. The precursor drive signals are amplified and impedance matched by amplifiers **114** and **116** to become the reference drive signal **118** and slave drive signal **120** that are routed to the reference cable **56** and the slave cable **66**. Preferably, a single ultrasound oscillator is used to produce the sine and cosine signals to stabilize phase and minimize phase sweeping, as per Eq. 4, to avoid oscillator drift and frequency tolerances.

[0059] Phase Match and Shifter **108** Implemented Using Phase Estimation:

[0060] The reference transducer **52** drive signal **118** is described as

$$\omega=2\pi f$$

$$\text{drive}_{reference}(t)=a_{reference}\sin\omega t$$

and the slave transducer **62** ϕ_{slave} phase shifted drive signal **120** as

$$\text{drive}_{slave}(t)=a_{slave}\sin(\omega t+\phi_{slave})$$

At the location of the sensor **72**, the reference ultrasound beam **58** and slave ultrasound beam **68** are described as

$$\text{sensor}_{reference}(t)=k_{reference}a_{reference}\sin(\omega t+\phi_{reference})$$

$$\text{sensor}_{slave}(t)=k_{slave}a_{slave}\sin(\omega t+\phi_{slave}+\phi_{slave})$$

where the k's represent the effects of amplifier and transducer gains and signal degradation due to attenuation. The ϕ's are the additional phases introduced by electronics (e.g. amplifier, cabling, piezo-electric actuator, . . .), and transducer positioning relative to the sensor. The superposition of these two intersecting transducer ultrasound beams produces a resultant signal described using complex mathematics as

$$j=\sqrt{-1}$$

$$e^{jx}=\cos x+j\sin x$$

$$sensor_{reference}(j\omega)=k_{reference}\,a_{reference}\,e^{j(\omega t+\varphi_{reference})}$$

-continued

$$sensor_{slave}(j\omega) = k_{slave}a_{slave}e^{j(\omega t+\phi_{slave}+\varphi_{slave})}$$

$$sensor_{resultant}(j\omega) = a_{resultant}e^{j(\omega t+\varphi_{resultant})}$$

$$a_{resultant}e^{j(\omega t+\varphi_{resultant})} = k_{reference}a_{reference}e^{j(\omega t+\varphi_{reference})} + k_{slave}a_{slave}e^{j(\omega t+\phi_{slave}+\varphi_{slave})}$$

with the associated phasor equation

$$a_{resultant}e^{j\varphi_{resultant}} = k_{reference}a_{reference}e^{j\varphi_{reference}} + k_{slave}a_{slave}e^{j(\phi_{slave}+\varphi_{slave})}$$

The resultant sinusoid magnitude is calculated as

$$\begin{aligned} a_{resultant} &= \left|k_{reference}a_{reference}e^{j\varphi_{reference}} + k_{slave}a_{slave}e^{j(\phi_{slave}+\varphi_{slave})}\right| \\ &= \sqrt{\begin{aligned}&[k_{reference}a_{reference}\cos\varphi_{reference} + k_{slave}a_{slave}\cos(\phi_{slave}+\varphi_{slave})]^2 + \\ &[k_{reference}a_{reference}\sin\varphi_{reference} + k_{slave}a_{slave}\sin(\phi_{slave}+\varphi_{slave})]^2\end{aligned}} \\ &= \sqrt{\begin{aligned}&(k_{reference}a_{reference})^2 + (k_{slave}a_{slave})^2 + \\ &2k_{reference}k_{slave}a_{reference}a_{slave}\cos(\varphi_{reference} - \phi_{slave} - \varphi_{slave})\end{aligned}} \end{aligned}$$

with proportional power

$$\text{power}_{resultant} \propto (k_{reference}a_{reference})^2 + (k_{slave}a_{slave})^2 2k_{reference}k_{slave}a_{reference}a_{slave}\cos(\phi_{reference} - \phi_{slave} - \phi_{slave}) \quad (5)$$

Eq. 5, a generalized version of Eq. 1, establishes that the power of the resultant is maximized when $\omega_{reference} - \phi_{slave} - \phi_{slave} = 0$ or

$$\phi_{slave} = \phi_{reference} - \phi_{slave} \quad (6)$$

[0061] As shown in FIG. **11**, one embodiment **150** of the phase match and shifter **108** uses the buffered ultrasound signal **98** magnitude to estimate, individually, the phases of the reference transducer beam **58** and slave transducer beam **68** at the sensor **72**. The desired slave phase ϕ_{slave} applied to the slave precursor drive signal **112** is determined based on Eq. 6. As illustrated in FIG. **6**, ϕ_{slave} does not have to be precisely known and ±45° is sufficient to contain 90% of the maximum power. This phase match and shifter **108** with phase estimation **150** includes two switches **152** and **154** to null the slave precursor drive signal or the reference precursor drive signal **110**. A phase estimator **156** responds to the buffered ultrasound signal, and the resulting phase estimate **158** is used by the estimate phase shifter **160** to generate the slave precursor drive signal **112**.

[0062] With only the reference transducer **52** active (reference switch **152** closed and slave switch **154** open), the sensor **72** ultrasound signal **94** represents only the reference beam **58** ultrasound signal, and the phase estimator **156** phase estimate **158** is that of the reference phase ($P_{reference}$ at the sensor site. With only the slave transducer **62** active (reference switch **152** open and slave switch **154** closed), the phase estimate is that of the net slave phase λ_{slave} at the sensor site including the current known slave phase shift: $\lambda_{slave} = \phi_{slave} + \phi_{slave}$. ϕ_{slave} is calculated as $\phi_{slave} = \lambda_{slave} - \phi_{slave}$ and the next ϕ_{slave} is calculated as $\phi_{slave} + \phi_{reference} - \lambda_{slave}$.

[0063] FIG. **12** presents a basic algorithm for calculating and implementing the slave phase adjustment. The loop timing ΔT is selected to sufficiently sample the beam phases to accommodate the 100 Hz or so transducer movement spectrum. At time zero, $\phi_{last} = \phi_{slave} = 0$ and all switches are closed so that the reference and slave drives are normally active. After each period ΔT, the slave switch **154** is opened (no slave drive) and the phase estimator **156** responds to the buffered ultrasound signal **98** to estimate its phase **158** representing $\phi_{reference}$ of the reference beam **58**. Following, the slave switch is closed, the reference switch **152** opened (no reference drive), and the phase estimator responds to the buffered ultrasound signal to estimate its phase representing λ_{slave} of the slave beam **68**. Following, the estimate phase shifter **160** calculates the desired $\phi_{slave} = \phi_{last} + \phi_{reference} - \lambda_{slave}$, $\phi_{last} = \phi_{slave}$, phase shifts the slave precursor drive **112** accordingly, and closes the reference switch for the next cycle.

[0064] Analog Phase Estimation: As those skilled in the art can attest, phase estimation **156** is a common activity in engineering and is performed using analog circuitry as follows. Given sin ωt and cos ωt, the products of these with the buffered ultrasound signal **98**, represented generally by a sin(ωt+ϕ), are formed as

$$\begin{aligned} x &= a\sin(\omega t + \phi) \\ p_{sin} &= x\sin\omega t \\ &= \frac{1}{2}a\cos\phi - \frac{1}{2}a\cos\phi\cos 2\omega t + \frac{1}{2}a\sin\phi\sin 2\omega t \\ p_{cos} &= x\cos\omega t \\ &= \frac{1}{2}a\sin\phi + \frac{1}{2}a\cos\phi\sin 2\omega t + \frac{1}{2}a\sin\phi\cos 2\omega t \end{aligned}$$

These products consist of a dc phase component on which is superimposed ac components having frequency 2ω. Simple low-pass filtering (LPF) of these products at below 2ω produces the sine and cosine components of the phase: ½ a cos ϕ and ½ a sin ϕ. The ratio of these values

$$\tan\phi = \frac{\sin\phi}{\cos\phi} = \frac{\frac{1}{2}a\sin\phi}{\frac{1}{2}a\cos\phi}$$

is the tangent of the phase angle, and phase is determined using the inverse tangent

$$\phi = \tan^{-1}\left(\frac{LPF(x\cos\phi)}{LPF(x\sin\phi)}\right)$$

[0065] A block diagram of an analog embodiment **170** of the phase estimator **156** is presented in FIG. **14***a*. Typically therapeutic ultrasound frequencies are in the 0.5-8 MHz range, and the two FIG. **14***a* multipliers and LPFs are implemented in hardware where the multiplier must handle signals at least twice that frequency (see the 2ω terms in the p_{sin} and p_{cos} equations above). At least a 50 MHz multiplier is preferable, and devices such as the Analog Devices AD835 is a 250 MHz dc-coupled four-quadrant multiplier suitable for this application. The LPF is preferably a simple op-amp or R-C circuit with break frequency set at a few KHz to capture the dc components of the multiplier outputs, and an analog-digital

converter takes the LPF outputs into a computer, or other calculating electronic device, for division and arc-tangent operations for phase calculation. The low frequency division and inverse tangent operations can be implemented with a device such as the Analog Devices AD538 400 KHz integrated circuit.

[0066] Digital Phase Estimation:

[0067] A digital embodiment of the phase estimator **156**, based on Least Squares using signal digitization, works to estimate the products of the signal magnitude and the cos ϕ and sin ϕ factors as described below.

[0068] Model the sensor signal as x=a sin(ωt+ϕ) and decompose it into

$$\begin{aligned} x &= a\sin(\omega t + \phi) \\ &= a\cos\phi\sin\omega t + a\sin\phi\cos\omega t \\ &= [\sin\omega t\ \cos\omega t]\begin{bmatrix} a\cos\phi \\ a\sin\phi \end{bmatrix} \\ &= \underline{f}(t)\underline{p} \end{aligned}$$

Form the least square cost function to be minimized with respect to a cos ϕ and a sin ϕ based on measurements of x, x*, taken at $t_1, \ldots, t_k$ as

$$J(\underline{p}) = \sum_{k=1}^{K} [x^*(t_k) - \underline{f}(t_k)\underline{p}]^2$$

solve this linear system using

$$\underline{p} = \left[\sum_{k=1}^{K} \underline{f}(t_k)^T \underline{f}(t_k)\right]^{-1} \sum_{k=1}^{K} x^*(t_k)\underline{f}^T(t_k)$$

and calculate phase as

$$\phi = \tan^{-1}\left(\frac{a\sin\phi}{a\cos\phi}\right)$$

[0069] This digital approach is alternately implemented as a Kalman filter and uses discrete state transition and measurement relationships to sequentially improve estimates of p as:

$$\underline{p}_{k+1} = \underline{p}_k$$

$$x(t_{k+1}) = \underline{f}(t_{k+1})\underline{p}_{k+1}$$

resulting in

$$\underline{k}_{k+1} = \frac{1}{\underline{f}(t_{k+1})\underline{P}_{k/k}\underline{f}^T(t_{k+1}) + \sigma^2_{measurement}} \underline{P}_k \underline{f}^T(t_{k+1})$$

$$\underline{p}_{k+1} = \underline{p}_k + \underline{k}_{k+1}\left[x^*(t_{k+1}) - \underline{f}(t_{k+1})\underline{p}_k\right]$$

$$\underline{P}_{k+1} = [I - \underline{k}_{k+1}\underline{f}(t_{k+1})]\underline{P}_k$$

-continued

$$\phi(t_{k+1}) = \tan^{-1}\left(\frac{a\sin\phi_{k+1}}{a\cos\phi_{k+1}}\right)$$

The $\underline{p}_0$ and its uncertainty covariance, $\underline{P}_0$, are initialized according a priori estimates, and $\sigma_{measurement}$ is the $\underline{x}^*$ measurement standard deviation.

[0070] Regardless of the phase estimator **156** technique, the transport delay to and from the sensor, due to the speed of sound and the distance between the transducers and the sensor, is considered. A simple manner to estimate this delay is to use a coarse estimated distances from the transducers to the beam intersection coupled with the speed of sound in the intervening tissue (TBL 1), and wait that time after changing one of the switches **152** and **154** before re-sampling the phase conditions.

[0071] Phase Shifting:

[0072] The estimate phase shifter **160** must be able to generate a variable phase version of the reference transducer drive signal **110** and, as those skilled in the art can attest, there are many ways to do this. If the ultrasound oscillator **100** works digitally by creating a sinusoid using a sequence of digital steps, shifting the steps creates a phase shifted version. If the ultrasound oscillator is analog, an all-pass filter shifts phase and not amplitude to create a phased shifted version.

[0073] Alternately, since sine **104** and cosine **106** versions of the oscillating signal are available for phase estimation **156**, a general phase delay function uses the decomposition

$$\sin(\omega t+\phi)=\sin\omega t\cos\phi+\cos\omega t\sin\phi$$

and an analog embodiment **180** of the estimate phase shifter **160** is illustrated in FIG. **14***b* where the multiplier stages use an analog multiplier component such as the Analog Devices AD835.

[0074] In addition to forming the phase shifted slave precursor drive signal **112**, the estimate shifter **160** performs the FIG. **12** algorithm and controls switches **152** and **154**, and the phase estimator **156** using hardware and software facilities.

[0075] Phase Match and Shifter **108** Implemented Using Power Maximum Seeking:

[0076] As shown in

[0077] Eq. 5, the optimum ϕ_{slave} is the value that maximizes power. As shown in FIG. **14** and FIG. **15**, a power maximum seeking embodiment **190** of the phase estimator and shifter **108** uses a dither approach to adjust ϕ_{slave} to maximize the power of the sensor **72** buffered ultrasound signal **98** without switches and without interrupting therapy with switch action. The dither approach, familiar to those skilled in the art, is similar to a gradient maximization scheme where the slave phase ϕ_{slave} is perturbed a small amount, the resulting power in the reported ultrasound signal is measured, and the phase controlled in the direction of increasing power. A basic algorithm is presented in FIG. **15**.

[0078] The maximum seeking phase match and shifter **190** perturbs the slave precursor drive signal **112** phase ϕ_{slave} while the power calculator **192** determines resulting buffered ultrasound signal **98** power **194**. As those skilled in the art can attest, power determination has many analog and digital solutions. Since absolute power is not required, only relative power, the preferred approach is to determine the mean value of the square of the incoming signal during a signal acquisition period. The acquisition period is preferably several cycles of the buffered ultrasound signal with, preferably, acquisition starting and stopping at the same position in the

cycle (e.g. a positive going zero crossing). The phase perturbation $\Delta\phi$ is on the order of 5°. Not shown in FIG. **15**, but understood from discussion above, the transducer to sensor transport delay must be dealt with by waiting the estimated period after changing ϕ_{slave} and before power is determined.

[0079] Intersecting Transducers Using Swept Phase Approach

[0080] Whereas the intersecting transducers using match phase approach **50** maximizes peak delivered power by establishing stationary interference patterns with maxima in the beam intersection **78**, the intersecting transducers using swept phase **200** avoids stationary interference patterns to mitigate wave cancellation, as seen in FIG. **8**. Like the phase matching mode, swept phase provides a power gain of 4× relative to tissue in the non-intersecting beams. Any of the three intersections of FIG. **3***b-d* apply, and swept phase does not require an ultrasonic sensor, although an optional temperature probe to monitor therapy progress, as per FIG. **1**, is considered. Preferably, the Fresnel-Fresnel interference pattern of FIG. **3***c* is used where therapy is performed in the cylindrical near field and the drive signal frequency f and transducer diameter D define the depth of therapy and divergence angle β used to dissipate ultrasound intensity beyond the target tissue. The drive signal frequency f and the diameter D of the transducer are used, as illustrated in TBL 2, TBL 3 and FIG. **5**, to define the divergence angle of the beams to controlling the rate of intensity dispersion, and the depth of therapy.

[0081] As illustrated in FIG. **16**, except for not requiring sensor **72** and using phase sweeping driver generator **202** rather than a phase matching driver generator **82**, the swept phase approach **200** is similar in description to the phase matching approach **50** of FIG. **9**.

[0082] FIG. **17** presents an embodiment **210** of the phase sweeping drive generator **202** using two ultrasound oscillators **100**. Based on Eq. 3, the first ultrasound oscillator **100**, operating at frequency **102** ω, generates sin ωt that is the precursor reference drive signal **110**, and the second ultrasound oscillator, operating at a slightly different frequency **102** $\omega+\phi_{slave}$, generates the $\sin(\omega t+\phi_{slave}t)$ phase swept slave precursor drive **112**. If ϕ_{slave} is a constant, a linearly swept phase is generated, and ϕ_{slave} can be varied for other affects. The accuracy of this embodiment is limited by the frequency accuracy of the two ultrasound oscillators.

[0083] FIG. **18** illustrates the preferred embodiment **220** of the phase sweeping drive generator **202** using a single ultrasound oscillator **100** to generate the reference precursor drive signal **110** and a phase sweeping phase shifter **222** to generate the slave precursor drive signal **112**. As illustrated in FIG. **19**, and based on the identity

$$\sin([\omega t+\phi_{slave}(t)]=\sin \omega t \cos [\phi_{slave}(t)]+\cos \omega t \sin [\phi_{slave}(t)]$$

an embodiment **230** of the phase sweeping phase shifter **222** uses a swept phase generator **232** to generate the sine **236** and cosine **234** functions of the time varying ϕ_{slave}. The cosine and sine values are provided by the swept phase generator **232**.

[0084] The $\phi_{slave}(t)$ sweep rate is on the order of a few hundred Hz, and FIG. **20** illustrates an embodiment **240** of the swept phase generator **232** using a low frequency oscillator **244** that linearly sweeps phase at rate ϕ_{slave} as per Eq. 3. Using frequency **242** ϕ_{slave}, the low frequency oscillator produces the sine **236** and cosine **234** values of the time varying phase $\phi_{slave}(t)=\phi_{slave}t$. If ϕ_{slave} is a constant, a linearly swept phase is generated, and ϕ_{slave} can be varied for other affects.

Satisfying the Objects of the Invention

[0085] The object of the invention was earlier state to provide a therapeutically effective ultrasound device that can go where HIFU cannot, is safer, less expensive, does not require an MRI, and handles larger incremental volumes. These objects are satisfied: the multi-beam ultrasound device:

[0086] is small and used within the body in the near vicinity of the target tissue, and can be inserted using minimally invasive methods;

[0087] is safer because is in the near vicinity of the target tissue and under manual control by the medical professional who can see bones or gas or other scattering obstructions;

[0088] conventional ultrasound transducer are used and does not require the complexity, expense, and size of the HIFU emitters and drive electronics;

[0089] an MRI is not required as the device is in the hands of the medical practitioner who can visibly guide its beams; and

[0090] larger incremental volumes are handled, the intersection of beams rather than the focus of a cone.

OTHER EMBODIMENTS

[0091] While several illustrative embodiments of the invention have been shown and described, numerous variations and alternate embodiments will occur to those skilled in the art. For example:

[0092] including more than two slave transducers;

[0093] reference and slave transducers arranged external to the patient surface;

[0094] the sensor incorporated within the reference or slave transducer;

[0095] using focused rather than unfocused transducers;

[0096] in addition to therapeutic applications, include industrial uses; and

[0097] selecting the transducer drive frequency and geometry in response to the desired depth of therapy as per FIG. **5**.

[0098] Such variations and alternate embodiments, as well as others, are contemplated and can be made without departing from the spirit and scope of the invention as defined in the appended claims.

What is claimed is:

1. An ultrasound device, comprising a plurality of acoustic transducers forming a plurality of acoustic pressure beams, where said beams are arranged to intersect and interfere and where their relative phases are controlled to enhance interference in a manner that increases the device interaction with the physical state of material at the intersection.

2. The ultrasound device of claim **1** including a sensor located at the intersection, said sensor having an output signal responsive to the acoustic pressure and where said relative phase control is in response to said signal.

3. The responsiveness to said signal of claim **2** includes estimating the phases of the plurality of beams at their intersection and adapting said relative phase control to make said phases equal.

4. The responsiveness to said signal of claim **2** includes estimating the power delivered by the plurality of beams at

their intersection and where said relative phase control is adapted to maximize said power.

5. The sensor of claim **2** is further responsive to the temperature at the intersection where said temperature is used to monitor said interaction with said physical state.

6. The sensor of claim **2** where said acoustic pressure responsive sensor is one of said plurality of acoustic transducers.

7. The ultrasound device of claim **1** where said relative phase control is by phase sweeping.

8. The ultrasound device of claim **7** where the plurality of acoustic transducers are driven by a distinct drive signals having distinct frequencies, and phase sweeping is by use of said different frequencies.

9. The ultrasound device of claim **1** where said transducer acoustic pressure beams are focused.

10. The ultrasound device of claim **1** where said intersection lies in the Fresnel-Fresnel zone, where said transducers are responsive to drive signals having a frequencies of operation, and where the effective depth of said interaction by the plurality of beams is selected by said frequencies and the geometries of said transducers in a manner to disperse their beam interaction beyond the intersection.

11. A method to increase the interaction of an ultrasound device, having a plurality of acoustic transducers forming a plurality of acoustic beams arranged to intersect and interfere, with material at the intersection comprising the step of controlling the relative phases of the beams to enhance said interference.

12. The method of claim **11** further comprising the steps

including a sensor located at the intersection, said sensor having an output signal responsive to the acoustic pressure; and

controlling the relative phase in response to said signal.

13. The method of claim **12** where the responsiveness to said signal includes estimation of the phases of the plurality of beams at their intersection and where said relative phase control strives to make said phases equal.

14. The method of claim **12** where the responsiveness to said signal includes estimating the power delivered by the plurality of beams at their intersection and where said relative phase control is adapted to maximize said power.

15. The method of claim **12** further including the step

adapting said sensor to further be responsive to the temperature at the intersection; and

using said temperature is to monitor said interaction with said physical state.

16. The method of claim **12** where said acoustic pressure responsive sensor is one of said plurality of acoustic transducers.

17. The method of claim **11** where said relative phase control is by phase sweeping.

18. The method of claim **17** further including the step of driving the plurality of acoustic transducers by distinct drive signals having distinct frequencies, and phase sweeping is by use of said different frequencies.

19. The method of claim **11** where said transducer acoustic pressure beams are focused.

20. The method of claim **11** further including the steps

arranging said intersection to occur in the Fresnel-Fresnel zone;

adapting said transducers to be responsive to drive signals having frequencies of operation; and

selecting the effective depth of said interaction by the plurality of beams by adapting said frequencies and the geometries of said transducers to disperse their beam interaction beyond the intersection.

* * * * *

专利名称(译)	多光束超声装置		
公开(公告)号	US20150141874A1	公开(公告)日	2015-05-21
申请号	US14/082541	申请日	2013-11-18
[标]申请(专利权)人(译)	WILSON KITCHENER CLARK		
申请(专利权)人(译)	WILSON，KITCHENER CLARK		
当前申请(专利权)人(译)	WILSON，KITCHENER CLARK		
[标]发明人	WILSON KITCHENER CLARK		
发明人	WILSON, KITCHENER CLARK		
IPC分类号	A61N7/02 A61B5/00 A61B5/01		
CPC分类号	A61N7/02 A61B5/01 A61N2007/0073 A61N2007/0078 A61B5/4836		
外部链接	Espacenet USPTO		

摘要(译)

提出了一种具有交叉光束的多光束超声装置，用于医疗和工业。多个超声波束根据它们在目标组织处的相位而相长和相消地干涉，并且该装置及其方法使用相位控制来在光束交叉点处增强强度。在许多实施例中，详细描述了两个：相位匹配，其中光束的相位被确定和控制为相等，以及相位扫描，其中光束的相位是有目的地变化的。